

Radiation damage in MgAl_2O_4

G. P. Summers

*Department of Physics, Oklahoma State University, Stillwater, Oklahoma 74074*G. S. White,* K. H. Lee,[†] and J. H. Crawford, Jr.*Department of Physics and Astronomy, University of North Carolina at Chapel Hill, Chapel Hill, North Carolina 27514*

(Received 3 July 1979)

Exposure of single crystals of MgAl_2O_4 to fast neutrons and to Van de Graaff electrons with energies in excess of 0.35 MeV introduces an optical-absorption band at 5.3 eV with a 1-eV half-width. This band can be partially bleached at temperatures as low as 40 K and a shoulder at 4.75 eV develops concurrently. This bleaching treatment also partially destroys a previously reported V -type absorption centered at 3.2 eV. Subsequent exposure to ionizing radiation destroys the 4.75-eV band and restores both the 5.3- and 3.2-eV bands to their original intensities. Since this behavior is analogous to the interconversion of F to F^+ centers in Al_2O_3 , it is concluded that the 5.3-eV band is the principal optical transition of the F center (two electrons trapped at an oxide-ion vacancy) and the 4.75-eV band is attributed to absorption by the F^+ center (one electron trapped at an oxide-ion vacancy). In electron-irradiated crystals the 5.3-eV absorption begins to anneal near 110°C and is about 90% destroyed upon isochronal annealing (10-min pulses) up to 355°C. Neutron-irradiated crystals behave similarly. Measurement of the threshold energy for damage by electrons at 77 K yields a displacement energy for the creation of O^{2-} interstitial-vacancy pairs of 59 eV. The defect yield drops off substantially with increasing temperature, and at room temperature the apparent O^{2-} displacement energy is 130 eV. Possible reasons for this strong temperature effect are discussed.

INTRODUCTION

Research on radiation-induced defects in various charge states in alkaline-earth oxides has been pursued with considerable success over the last dozen years or so.¹ Recently, the conceptual tools and experimental methods developed in these studies have been applied with varying degrees of success to oxides with a more complicated crystal structure such as $\alpha\text{-Al}_2\text{O}_3$ and MgAl_2O_4 . Although identification of trapped-hole (V -type) optical transitions in Al_2O_3 , based on infrared absorption² and electron-spin-resonance (ESR) measurements, is on firm footing,³⁻⁵ the absence of a convenient ESR signal⁶ from the paramagnetic F^+ center (a single electron trapped on an anion vacancy) has hampered direct identification of the optical transition of this center. Similarly, ESR signals from both electron and hole centers in MgAl_2O_4 crystals are either so complex or so weak that this means of identifying the defects responsible for optical bands has so far proved ineffective.⁷ Therefore the origin of the optical bands has had largely to be deduced by analogy with the behavior of similar centers in alkaline-earth oxides. In MgO , for example,^{1,8} ESR and magnetic-circular-dichroism (MCD) measurements have located both the F^+ band and the F band (the optical transition of the center composed of two electrons trapped on an O^{2-} vacancy) near 5.0 eV. In Al_2O_3 the F^+ center, identified through the polarized excitation spectrum of its 3.8-eV emission band, absorbs

at 4.8, 5.4, and ~ 6 eV, whereas the F center absorbs at 6.1 eV and luminesces near 3.0 eV.⁹⁻¹³

MgAl_2O_4 has a melting point intermediate between that of its constituents, i.e., 2135 °C as compared to 2800 °C for MgO and 2047 °C for Al_2O_3 . Its absorption edge⁷ of 7.75 eV is comparable to that of its parent oxides. The spinel structure is characterized by two types of cation sites: octahedral for the trivalent cations and tetrahedral for the divalent cations, though some mixing of cations over these sites is common.^{14,15} Hence a wide variety of defect configurations and charge states is possible, including misplacement of cations (antistructure defects).

Some of the effects associated with a change in charge state of defects and impurities can be readily explored using ionizing radiation. In an earlier investigation,¹⁶ exposure to ^{137}Cs γ rays produced a broad absorption band centered near 3.2 eV and at the same time drastically reduced absorption initially present in bands at 4.9 and 6.4 eV. The latter bands coincide in energy with Fe^{3+} charge-transfer absorptions in Al_2O_3 crystals reported by Tippens.¹⁷ Since Fe was a major contaminant of these crystals and since the Al-O spacing in spinel is very close to that in Al_2O_3 , it seems reasonable to conclude that these bands are also associated with Fe^{3+} impurity in MgAl_2O_4 and that the 3.2-eV band is due to a V -type center, i.e., a hole trapped in the form of an O^- adjacent to a site deficient in positive charge. Optical and thermal bleaching of the 3.2-eV band result in a

one-to-one restoration of the Fe^{3+} bands.

Bunch¹⁸ has reported that bombardment of spinel crystals with 14-MeV neutrons introduced a prominent band at 5.3 eV, which he identifies as an *F*-type band on the basis of a Mollwo-Ivey-type relationship. This assignment is strengthened by thermochemical studies¹⁹ which demonstrate that the 5.3-eV band can be produced both additively, by heating spinel crystals in either Mg or Al metal vapor, and extractively, by heating near the melting point in a reducing atmosphere. In the following account we summarize our studies of optical-absorption bands in spinel which had been irradiated with reactor-spectrum neutrons or energetic electrons (>0.35 MeV). These include optical- and thermal-bleaching experiments and a determination of threshold energies for their creation by electron bombardment.

EXPERIMENTAL METHODS

The MgAl_2O_4 single crystals were obtained from Union Carbide Corporation. A chemical assay carried out by Johnson and Mathey analysts revealed that the primary impurity was iron present to the extent of 76 ppm in one set of samples and to 20 ppm in another. Smaller amounts of other impurities, e.g., 22-ppm Cu and 4-ppm Cr in the first set and 1-ppm Cu and 3-ppm Cr in the second, were also reported. Neutron irradiation was performed in the North Carolina State University Pulsar reactor which has a flux of reactor spectrum neutrons of 10^{13} cm^{-2} sec^{-1} . Electron irradiations were carried out at two locations, using the 2-MeV Van de Graaff at Chapel Hill and the 0.5-MeV Van de Graaff at AERE Harwell. At the first location, beam currents up to ~ 100 μA were employed and the specimens were cooled with a high flow of water in direct contact with the specimen. Since in this setup the electron beam penetrated two thin metal walls and ~ 1 mm of water before reaching the specimen, there was appreciable degradation of the incident beam energy. In the AERE setup the specimen was attached to a cold finger extending from a liquid-nitrogen cryostat and was exposed directly to the electron beam. This second arrangement was much better suited to determine the threshold energies directly without corrections for energy degradation and could be used, provided current densities did not exceed ~ 10 $\mu\text{A}/\text{cm}^2$.

EXPERIMENTAL RESULTS: THE 5.3-eV BAND

Exposure of MgAl_2O_4 crystals to particles with sufficient energy to displace lattice ions via elastic collisions results in the 5.3-eV absorption band reported by Bunch.¹⁸ The effect of an ex-

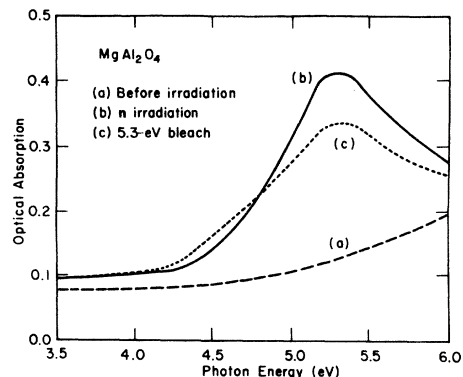


FIG. 1. Optical absorption in single-crystal MgAl_2O_4 introduced by an exposure of 1×10^{16} reactor neutrons cm^{-2} . Curve *a*, before irradiation; curve *b*, after irradiation at $\sim 40^\circ\text{C}$; curve *c*, after bleaching with 5.3-eV light at room temperature (the specimen was exposed to a beam of 5.3-eV photons from a high-intensity monochromator until no further change was observed).

posure of 3×10^{16} reactor-spectrum neutrons cm^{-2} at $\sim 40^\circ\text{C}$ is shown in Fig. 1, where the absorption coefficient α is plotted against photon energy. The 5.3-eV band completely dominates the spectrum. It is unaffected by exposure to visible light and has a width at half-maximum of ~ 1.0 eV. Though not shown in this figure, the 3.2-eV *V*-type band is detectable but quite small. Bombardment with 1.75-MeV electrons produces the same 5.3-eV band (same width and position), but the 3.2-eV band development is more prominent. However, growth curves for these bands produced by 1.75-MeV electrons, shown in Fig. 2, show that the 3.2-eV band attains at least half of its intensity almost immediately and that its subsequent growth is relatively very slow. On the other hand, the 5.3-eV band grows with a substantial rate over the whole exposure range, though the onset of saturation is evident at higher exposures. Therefore it appears that the 5.3-eV band requires defect creation by a displacement process as reported by Bunch,¹⁸ while most, if not all, of the centers responsible for the 3.2-eV band are apparently already present

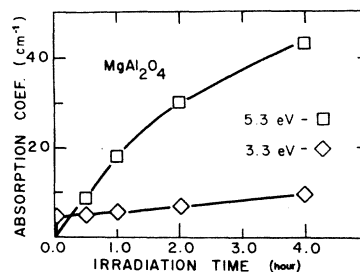


FIG. 2. Buildup of coloration at room temperature due to 1.75-MeV electron bombardment of MgAl_2O_4 single crystals. Absorption intensity at both 5.3 and 3.3 eV.

and require only a charge-state change to become observable. This behavior is consistent with earlier observations of the effect of γ irradiation on MgAl_2O_4 , which indicated that the 3.2-band is associated with holes trapped at some site deficient in positive charge already present in the crystal.

OPTICAL BLEACHING

Light absorbed in the 5.3-eV band causes partial bleaching and the appearance of a shoulder at 4.75 eV, as shown in Fig. 3, for an electron-bombarded crystal. The bleaching can be carried out at either room temperature or at temperatures as low as 40 K. Another consequence of excitation in the 5.3-eV band is the partial loss of the V -type band at 3.2 eV. It was also noted that the extent of bleaching was specimen-dependent and that some specimens, while susceptible to bleaching at 77 K, were not strongly affected at room temperature. Electron-bombarded crystals were more sensitive to bleaching than neutron-bombarded ones. The effect of a 5.3-eV bleach for a neutron-irradiated crystal at room temperature is shown in curve c, Fig. 1. Exposure to a small dose of x rays or γ rays at room temperature completely restores the 5.3-eV band and erases the 4.75-eV shoulder. These observations are all consistent with the view that optical excitation of the defect responsible for the 5.3-eV absorption causes it to lose an electron which annihilates a hole in a V -type center. The specimen dependence of the bleaching efficiency and the fact that low-temperature bleaching is more effective than room-temperature indicate that the 4.75-eV band is not associated with the trapping of electrons released during the bleaching process, but rather is very likely due

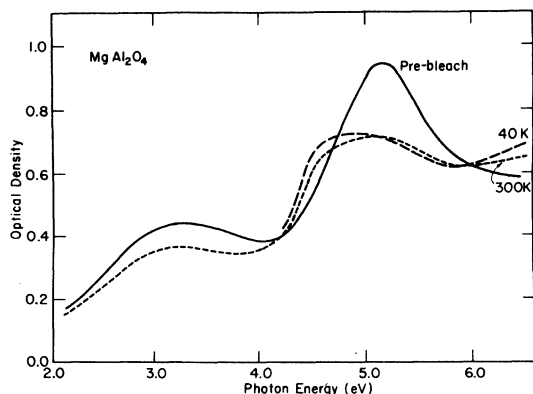


FIG. 3. Effect of bleaching with 5.3-eV light on the optical absorption spectrum of MgAl_2O_4 previously exposed to 0.5-MeV electrons. The effect of bleaching at both 40 K and room temperature is shown. Optical density measurements were made at the bleach temperature.

to a new charge state of the defect undergoing photoionization. This is just the behavior expected if the 5.3-eV band were due to F -center excitation and the 4.75-eV absorption were associated with the F^+ center. A short exposure to ionizing radiation restores the 5.3-eV band intensity and eliminates the 4.75-eV shoulder through restoration of the original charge state. Similar behavior is exhibited by Al_2O_3 upon bleaching,⁹⁻¹³ except that, because the lower symmetry of the oxygen vacancy site splits the excited state, there are three F^+ bands rather than one.

Another piece of evidence which is in accord with this identification is that when an electron-bombarded crystal is kept in the dark for several days, the 4.75-eV shoulder develops on the 5.3-eV band. It is known from thermoluminescence studies¹⁶ on γ -irradiated specimens that holes are thermally released from V -type centers at temperatures below 100 °C even though the main peak lies at 195 °C. Therefore, we expect holes escaping from such shallow traps to be captured by F centers producing a corresponding number of F^+ centers.

In view of these results, we conclude that the 5.3-eV band in spinel is associated with the F center and the 4.75-eV band belongs to the F^+ center. As mentioned above, this conclusion is supported by the fact that the same 5.3-eV band can be created by thermochemical treatment¹⁹ designed to introduce a stoichiometric excess of the metallic constituent and, hence, also F centers.

THERMAL ANNEALING

Isochronal annealing (10-min pulses at successively higher temperature) was carried out on both electron- and neutron-bombarded crystals. It was found that the 5.3-eV peak noticeably decreases when the temperature reaches 80 °C, but that this decrease can be fully restored by a short exposure to ionizing radiation (x rays in this case), so long as the temperature does not exceed 110 °C. Therefore thermal bleaching at these lower temperatures is presumably associated with holes released from V -type centers. To avoid confusing such electronic effects with the loss of centers by interstitial-vacancy recombination during the anneal, the specimens were given a 20-min exposure to x rays after each annealing pulse to repopulate both electron and hole centers. Thermal destruction of centers responsible for the 5.3-eV band sets in above 110 °C and by 355 °C is 90% complete. Annealing to temperatures above 1000 °C is necessary to eliminate the remaining 10% of this band. Typical spectra for an electron-bombarded crystal, after isochronal annealing pulses at the

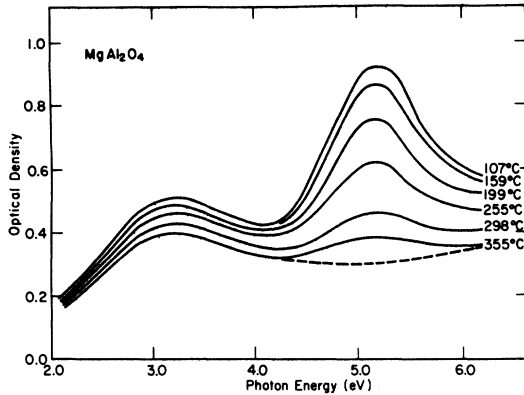


FIG. 4. The effect of isochronal annealing (10-min annealing pulses) on the optical absorption spectrum of an electron-bombarded MgAl_2O_4 crystal. The curves were measured after successive anneals up to the indicated temperature. After each annealing pulse the crystal was given a 20-min x-ray exposure to repopulate F - and V -type centers. The dashed curve shows the effect of x irradiation on a comparison specimen which had not been exposed to electrons.

indicated temperatures, are shown in Fig. 4. Defects in neutron-bombarded crystals exhibited comparable thermal instability, except that virtually all of the 5.3-eV band was removed by annealing to 400 °C.

In Fig. 4 it is also evident that loss in the 5.3-eV band is accompanied by loss in the 3.2-eV trapped-hole band. It is not clear whether this loss of absorption is caused by thermal destruction of V -type centers or whether loss of the electron-trapping capacity of the F -type centers simply reduces the concentration of holes available to populate hole centers upon exposure to ionizing radiation. Experience with specimens containing ~70-ppm Fe impurity¹⁶ supports the latter view, since it was found that γ irradiation virtually eliminated the 4.8- and 6.4-eV absorption bands due to Fe^{3+} . Evidently, the concentration of hole-trap centers is greater than that of the Fe^{3+} impurity so that as many holes as necessary to balance the concentration of trapped electrons can be accommodated. Another indication of the high concentration of hole traps is the strong afterglow immediately after γ irradiation.¹⁶ This phosphorescence is dominated by 4.8-eV emission which has been attributed to electron capture by occupied hole traps, i.e., V -type centers. A similar emission at 4.95 eV has been found to result from the same recombination process in x-irradiated MgO .²⁰ Hence, electrons released at a low rate, at room temperature, from shallow traps, evidently recombine with trapped holes, resulting in a decrease of the 3.2-eV band intensity. Both of these observations suggest that it is the concentration of

trapped electrons which controls the amplitude of the 3.2-eV absorption. If the hole-trap concentration is indeed in excess of that required to balance the concentration of trapped electrons at room temperature, it is not possible to state whether additional V -type centers are created by either electron or neutron bombardment. Therefore the growth of the 3.2-eV band during electron bombardment (Fig. 2) should probably be interpreted as reflecting an increase in the concentration of deep electron traps resulting from the displacement of lattice ions, e.g., O^{2-} , rather than creation of additional V -type centers.

The isochronal annealing behavior observed in Fig. 4 exhibits no sharp recovery stage but rather a nearly uniform rate of annealing over the temperature interval from 110 °C to 355 °C. Similar annealing behavior is exhibited by neutron-bombarded crystals and suggests a distribution of activation energies, rather than a unique one which would be expected if, say, the rate-determining step were due to the motion of a vacancy or an interstitial. Therefore it is likely that the breakup of interstitial clusters dominates the recovery process and the range of energies required to dislodge an oxygen interstitial is larger than the motion energy for the interstitial. It is noted that similar isochronal annealing results have been obtained on neutron-irradiated MgO (Ref. 21) and Al_2O_3 .^{22,23}

DAMAGE-THRESHOLD MEASUREMENTS

If, as assumed here, the 5.3-eV absorption band is due to the F center, it should be possible to use this absorption band as an index of the displacement process and thus to determine the threshold energy for creating anion vacancies by electron bombardment. From a knowledge of the minimum electron energy capable of creating stable anion interstitial-vacancy pairs, it is possible to determine the so-called displacement energy E_d from the relativistic energy-transfer equation for the threshold case:

$$E_d = 2(E_{\text{th}} + 2mc^2)/Mc^2, \quad (1)$$

where E_d is the maximum kinetic energy transferred to an atom (ion) of mass M in a collision with an electron whose energy E_{th} is just sufficient to produce a change in the indexing property. In Eq. (1) m is the electron rest mass and c is the speed of light. A straightforward way to determine E_{th} is to expose a specimen to a prescribed fluence of electrons of energy E and increase E stepwise from some subthreshold value to a value in excess of E_{th} . Since the damage cross section near threshold is²⁴

$$\sigma_d(E) \propto (T_m/E_d) - 1, \quad (2)$$

where T_m is the maximum kinetic energy imparted in the collision, $\sigma_d(E)$ vanishes when $T_m = E_d$ or $E = E_{th}$. Therefore, by extrapolating back to no change in the indexing property, the value of E_{th} , and hence E_d , may be obtained. When T_m is significantly larger than E_d , a more exact extrapolation due to Seitz and Koehler²⁴ can be used; i.e., one can fit the normalized displacement cross section to the experimental points of the property-change variation versus incident electron energy.

In our case the 5.3-eV band was used as the index of O^{2-} displacements. E_d was determined for electron bombardment at both 77 and 300 K using two rather different sample holders. At 77 K the thermal conductivity of spinel was high enough for the electron-beam intensities employed ($\sim 10 \mu A/cm^2$) to permit the sample to be attached to a liquid-nitrogen cold finger located in the Van de Graaff vacuum. After a fluence of 5×10^{17} electrons cm^{-2} , the sample was warmed to room temperature, at which the electron-hole recombination phosphorescence¹⁹ was allowed to decay for ~ 1 h and then the optical-absorption spectrum was measured. The 5.3-eV band first appeared with measurable intensity after irradiation with 0.35-MeV electrons. Extrapolation to zero optical density after subsequent irradiation at higher energies gave $E_{th} = 0.325$ MeV, which according to Eq. (1) corresponds to $E_d = 59$ eV. Just above threshold the defect production rate is relatively small, but if the electron-beam energy is increased to 0.5 MeV, the production rate is much higher and a fluence of 2.5×10^{18} electrons cm^{-2} produced an optical density of 0.4. Assuming an electron penetration depth of ~ 0.2 mm before the electron energy falls below threshold and an oscillator strength of ~ 1 for the 5.3-eV band, Smakula's equation can be used to estimate that about 30 incident electrons on the average produce one oxygen vacancy at 77 K. The number of defects produced is directly proportional to the electron fluence up to an optical density of 0.2, which, using the above penetration depth, corresponds to an absorption coefficient of about $30 cm^{-1}$. At high fluences the defect production rate decreases slightly. For irradiations at 300 K the defect production rate was at least a factor of 6 below that at 77 K for an incident electron energy of 0.5 MeV.

When threshold measurements were carried out at room temperature using higher beam currents ($\sim 100 \mu A/cm^2$) and water cooling, the results shown in Fig. 5 were obtained. Before striking the samples, the electron beam had to penetrate ~ 0.3 mm of window material (aluminum and brass) and a 1-mm layer of water. Hence considerable

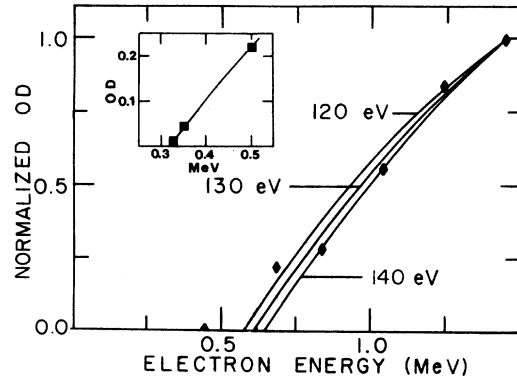


FIG. 5. Optical density (OD) at 5.3 eV as a function of incident electron energy near room temperature. Each point was measured after 2×10^{18} electrons cm^{-2} . The indicated electron energy was corrected for energy loss in window material and 1-mm layer of cooling water using the known stopping power of these substances. The insert shows the optical density measured at room temperature, which was introduced at 77 K by 5×10^{17} electrons cm^{-2} . For these measurements the sample was held in the accelerator vacuum. The sample thickness was 1 mm.

degradation of the beam energy occurred before the incident electrons reached the specimen. The energy values of Fig. 5 were corrected both for the energy lost by the electrons in traversing the layers of window material and for the finite thickness of the specimen by using known stopping powers.²⁵ Because of inherent uncertainties in these corrections and straggle in the beam, the effective incident-electron energies are not so well defined as in the low-temperature threshold measurements. Therefore, to verify the validity of this approach, the threshold energy of MgO was determined in the same holder by the same procedure and the value of 59 eV was obtained, which is in excellent accord with a previously reported measurement at 77 K.²⁶ The solid lines of Fig. 5 were calculated using the $\sigma(E)$ relation of Seitz and Koehler for E_d 's of 120-, 130-, and 140 eV. The best overall fit to the data is given by $E_d = 130$ eV, a value over twice as large as obtained from the low-temperature measurements. However, as can be seen from Fig. 5, the data points trail off toward lower electron energies at small values of 5.3-eV band intensities.

The usual interpretation of displacement-energy measurements using incident electrons is that E_d represents the minimum energy imparted to a lattice atom or ion in an elastic collision, which will result in the formation of an interstitial-vacancy pair. As such E_d is expected to have a definite, fixed value. However, it is obvious that, since in our case the property indicating permanent damage

is measured subsequent to the irradiation, we are concerned with both the effect of the radiation conditions and the interval between irradiation and measurement on the stability of the interstitials and vacancies. Unless the defects are stable against recombination, no damage will be indicated. In our case low-temperature irradiation gave the lowest value of E_d ; therefore what happens in the interval between irradiation and measurement is not nearly as important as the effect of irradiation conditions on the stability of interstitial-vacancy pairs immediately after creation. Hence in the usual experimental situation E_d is determined by the lowest value of T_m , which results in stable damage rather than that necessary simply to displace an atom to an interstitial site. Consequently, the stable-damage configuration is expected to be more complex than simple interstitial-vacancy pairs.

In close-packed structures one expects the activation energy of interstitials to be rather small and, indeed, in alkali halides there is evidence that interstitial halide ions are quite mobile.²⁷ One might also expect a similar high mobility of interstitial oxygen ions in the spinel lattice. Because of the instability of O^{2-} in the absence of the stabilizing Madelung field (the electron affinity of the second electron is -9 eV), the displaced oxygen is expected to lose immediately one electron and become O^- . This small ion should move readily through the lattice either directly or by an "electronic" interstitial mechanism, i.e., exchange both position and charge with an on-site ion, even at low temperatures. With such a high mobility the probability of recombination of an interstitial with some vacancy would be quite large. Thus creation of stable oxygen vacancies requires the trapping of the corresponding interstitials. At low temperature rather shallow traps would suffice to provide a nucleation site for interstitial clusters, i.e., to trap a single O^- which could then capture additional O^- ions to form a small cluster stable at room temperature.

At higher temperatures (~ 300 K) such trapping sites, if shallow enough, would be relatively ineffective, so that a drastic reduction of the yield of anion vacancies for incident-electron energies

near E_d would occur. However, if the creation rate of interstitial-vacancy pairs is high enough, homogeneous nucleation through the interaction of two O^- becomes increasingly probable. A sufficiently enhanced production rate for homogeneous, second-order nucleation might well result from higher incident-electron energies. The result would be a production rate versus electron energy behavior like that of the data points of Fig. 5.

An alternative model for the apparently higher E_d at room temperature involves the creation of a more complex, more stable type of damage at the outset. For example, multiple displacements by a single electron- O^{2-} -ion collision may produce a damage configuration which stabilizes the interstitial component as well as the vacancy. This creation mechanism would lead to a second, high-yield threshold; such effects have been reported in the case of silicon.²⁸ The data points of Fig. 5 could be interpreted as indicating a two-threshold situation. It should be possible to distinguish between these two alternatives by using several different beam intensities, since second-order homogeneous nucleation would be favored by the higher intensities, whereas the complex damage model would depend only on the energy of the incident electrons and not on the flux.

ACKNOWLEDGMENTS

The authors express their appreciation to J. M. Bunch of Los Alamos Scientific Laboratory for providing the high-purity (low iron content) specimens used in this research. We also wish to thank the staff of the Nuclear Service Laboratory at North Carolina State University for providing neutron irradiations. Support for this work by the Department of Energy at both the University of North Carolina and Oklahoma State University is gratefully acknowledged. Several of us (G.S.W., K.H.L., and J.H.C.) wish to thank the University Research Council for providing certain items of equipment used in these studies. One of us (G.P.S.) wishes to thank the Atomic Energy Research Establishment, Harwell, England, for their hospitality during research leave. Electron irradiations at Harwell were performed with the assistance of R. Dawson.

*Present address: National Bureau of Standards, Washington, D. C. 20234.

†Present address: Dept. of Physics, Michigan Technological Univ., Houghton, Michigan 49931.

¹B. Henderson and A. E. Hughes, in *Point Defects in Solids*, edited by J. H. Crawford and L. M. Slifkin (Plenum, New York, 1972), Vol. 1, Chap. 7.

²T. J. Turner and J. H. Crawford, Jr., *Solid State*

Commun. **17**, 167 (1975).

³F. T. Gamble, R. H. Bartram, C. G. Young, O. R. Gilliam, and P. W. Levy, *Phys. Rev.* **134**, A589 (1964).

⁴K. H. Lee, G. E. Holmberg, and J. H. Crawford, Jr., *Solid State Commun.* **20**, 183 (1976).

⁵K. H. Lee, G. E. Holmberg, and J. H. Crawford, Jr., *Phys. Status Solidi* **39a**, 669 (1977).

- ⁶S. Y. La, R. H. Bartram, and R. T. Cox, *J. Phys. Chem. Solids* **34**, 1079 (1973).
- ⁷G. S. White, Ph.D. thesis, University of North Carolina at Chapel Hill, 1978 (unpublished).
- ⁸B. Henderson and J. E. Wertz, *Defects in the Alkaline Earth Oxides* (Taylor and Francis, London, 1977).
- ⁹K. H. Lee and J. H. Crawford, *Phys. Rev. B* **15**, 4065 (1977).
- ¹⁰B. D. Evans, H. D. Hendricks, F. D. Bazzarre, and J. M. Bunch, in *Ion Implantation in Semiconductors*, 1976, edited by F. Chernow, J. Borders, and D. Brice (Plenum, New York, 1977).
- ¹¹B. D. Evans and M. Stapelbrock, *Phys. Rev. B* **18**, 7089 (1978).
- ¹²B. G. Draeger and G. P. Summers, *Phys. Rev. B* **19**, 1172 (1979).
- ¹³K. H. Lee and J. H. Crawford, *Phys. Rev. B* **19**, 3217 (1979).
- ¹⁴G. E. Bacon, *Acta Crystallogr.* **5**, 684 (1952); E. Stoll, R. Fischer, W. Hälg, and G. Maier, *J. Phys.* **25**, 447 (1964).
- ¹⁵V. Schmocker, H. R. Boesch, and F. Waldner, *Phys. Lett.* **40A**, 237 (1972).
- ¹⁶G. S. White, K. H. Lee, and J. H. Crawford, *Phys. Status Solidi* **42A**, K137 (1977).
- ¹⁷H. H. Tippins, *Phys. Rev. B* **1**, 126 (1970).
- ¹⁸J. M. Bunch, *Phys. Rev. B* **16**, 724 (1977).
- ¹⁹G. S. White, K. H. Lee, and J. H. Crawford, *Appl. Phys. Lett.* **35**, 1 (1979).
- ²⁰K. H. Lee and J. H. Crawford, *J. Lumin.* **20**, 9 (1979).
- ²¹Y. Chen, R. T. Williams, and W. A. Sibley, *Phys. Rev.* **182**, 960 (1969).
- ²²P. W. Levy, *Discuss. Faraday Soc.* **31**, 118 (1961).
- ²³T. J. Turner and J. H. Crawford, *Phys. Rev. B* **13**, 1735 (1976).
- ²⁴F. Seitz and J. S. Koehler, *Solid State Phys.* **2**, 307 (1956).
- ²⁵M. J. Berger and S. M. Seltzer, *Nat. Acad. Sci.*, Pub. No. 1133 (1964).
- ²⁶Y. Chen, D. L. Trueblood, O. E. Schow, and H. T. Tohver, *J. Phys. C* **3**, 2501 (1970).
- ²⁷E. Sonder and W. A. Sibley, in *Point Defects in Solids*, edited by J. H. Crawford and L. M. Slifkin (Plenum, New York, 1972), Vol. 1, p. 235.
- ²⁸H. J. Stein and F. L. Vook, in *Radiation Effects in Semiconductors*, edited by F. L. Vook (Plenum, New York, 1968), p. 115.